Thermionics, Thermoelectrics, and Nanotechnology

New possibilities for old ideas.

AMIR H. KHOSHAMAN, HARRISON D.E. FAN, ANDREW T. KOCH, GEORGE A. SAWATZKY, AND ALIREZA NOJEH

Digital Object Identifier 10.1109/MNANO.2014.2313172
Date of publication: 2 May 2014

THE TERM *SOLAR CELL* USUALLY brings photovoltaics to mind. Indeed, the direct conversion of sunlight to electricity has dominated the realm of solar-energy harvesting for the past 50 years. However, researchers have now begun to re-evaluate the possibilities of thermionic and thermoelectric energy conversion because of some of their attractive features. These processes involve the conversion of heat to electricity, or light to heat to electricity, and have been investigated for over a century. Advances in nanoscale materials and fabrication techniques have now opened new doors for the application of these effects.

The resurgence of interest in these areas is mainly because of two reasons. First, the ever-increasing amount of waste heat generated and the need for alternative, clean energy sources has provided a new impetus for seeking effective ways of capturing this abundant source of energy. Second, advances in micro-/nanotechnologies have created opportunities for addressing some of the fundamental challenges that have plagued these devices since their inception.

For example, the workfunction of the materials used in thermionic converters has a strong impact on the device efficiency. Nanomaterials present a new avenue for engineering structures with low workfunction that could still be stable at the high operating temperatures involved. Device dimensions and interelectrode spacing are other critical factors. Here, again, micro-/nanotechnology enables previously unattainable dimensional control. Being that sunlight is a rich source of clean energy, it is highly desirable to be able to harvest it using efficient heat engines that do not involve sophisticated mechanics and moving parts. Thermionic and thermoelectric generation are excellent candidates for this purpose. However, reaching the required operational temperature is far from trivial due to the issues related to heat spread in the conductive electrodes of traditional devices. Recently, it has been shown that carbon nanotubes (CNTs) can be used as electrodes that, while being electrically conductive, can effectively trap heat and attain very high temperatures with low incident optical intensities, thus creating a new path for light-activated thermionics. Hence, some of the unique properties of nanostructures may offer new solutions to issues once thought insurmountable, such as the intricate relationship between electrical and thermal conductivity in metals.

In this article, we review the basics of thermionic and thermoelectric conversion. The important factors involved in optimizing the performance of converters based on these mechanisms are then discussed. In each case, we describe examples of solutions offered by micro-/nanostructures.

THERMIONIC CONVERSION

THE BASICS

A photovoltaic cell relies on the excitation of electrons through the absorption of photons and the subsequent spatial separation of electrons and holes. Fundamentally, the excitation and separation of electrons and holes does not necessarily have to be induced by light. For example, another way to excite electrons to higher energy levels is by heating the material. A thermionic energy converter (TEC) converts heat directly into electric power by means of thermionic electron emission, thus acting as an electric heat engine and without using moving parts like steam turbines. Typically, TECs are comprised of two main electrodes, as depicted in Figure 1.

The electrons are thermionically emitted from the hot electrode (emitter or cathode) into a vacuum (or some other medium), traverse the interelectrode distance because of their kinetic energy, and, eventually, are collected at the cold electrode (collector or anode). A negative charge thus builds up on the collector, gradually hindering further electron collection, until, eventually, the net electron flux between the electrodes becomes zero. If the external circuit is completed by connecting an electric load between the two

1932-4510/14/$31.00©2014IEEE

electrodes, the charge gathered at the collector will flow back to the emitter through the load, generating a steady-state output voltage and current.

Thermoelectric conversion is, in essence, similar to thermionic conversion, but without a vacuum gap separating the emitter and collector. Although thermoelectric effects were first discovered in metals, modern-day thermoelectric devices consist of semiconducting p-n junctions. In the Seebeck effect, both electrical contacts to the load are cooled, and the junction is kept at a higher temperature than the contact ends. If the temperature gradient is increased, the charge carriers can more readily surmount the junction potential barrier. The electrons travel from the n- to p-layer, and the holes from the p- to n-layer, resulting in an electromotive force. Alternatively, when a current passes from one material to the other, the kinetic energy of the electrons is changed, and the difference appears as heating or cooling at the junction; this is the related, but opposite, Peltier effect. We will discuss the thermoelectric effect in more detail later in this article.

Thermionic conversion may be viewed as a thermodynamic steam engine cycle that uses electrons as the working fluid. In a TEC, the emitter can be thought of as the electron boiler, while the collector is

IMAGE COURTESY OF FREEIMAGES/ALDIAZ

the electron condenser, leading to an electrical pressure (potential) gradient across a load. This will produce work similar to that done by vapor pressure in steam engines. In the ideal case, the overall system efficiency approaches the Carnot efficiency, since electron evaporation may be considered a reversible process, and the temperatures of the hot and cold electrodes may be assumed to be constant during the process. Additionally, irreversible mechanisms such as friction and turbulence are smaller compared to the situation in engines working with fluids. The thermionic current can be described by the Richardson–Dushman equation. This equation is found by summing up the contributions of all electrons having a velocity component normal to the emission surface and outward, assuming Fermi–Dirac statistics. By introducing several approximations, which are valid in most practical applications, the overall result is [1]

$$J = A^{*} T^{2} \exp\left(\frac{-\phi}{k_B T}\right),$$

where J is the current density, T is the absolute temperature, ϕ is the workfunction of the material, k_B is the Boltzmann constant, and A^{*} is the apparent emission constant of the material.

A number of early landmark efforts laid down the foundations of TEC technology. Although the quantitative description of thermionic emission was first presented by Richardson in 1902, the discovery of this phenomenon by Edison can be traced back to as early as 1885. Nonetheless, the earliest practical demonstrations of thermionic emission for energy conversion purposes emerged in the mid-1950s, when breakthroughs occurred in the technologies of high-temperature-stability electrodes and powerful heat sources [2]. The interelectrode gaps of about 100 μm in these TECs were formed by means of precision machining. These devices achieved efficiencies of 10–15% [3] and were subsequently used as power sources for space missions in the following two decades. However, the inherent electronic efficiency of a TEC, or the efficiency that strictly corresponds to the electronic processes under ideal electronic transport conditions, is much higher. In principle, this conversion efficiency can approach 90% of a reversible heat engine (the Carnot efficiency) [3], which can reach values of more than 60% under ideal conditions.

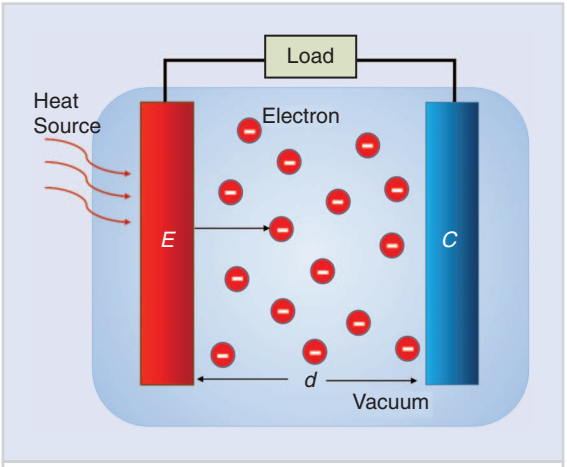

FIGURE 1 A schematic of a vacuum TEC: E is the emitter electrode, C is the collector electrode, and d is the interelectrode distance. Electrons inside the gap constitute the space-charge cloud. The device uses thermal energy from the heat source to deliver electric power to the load.

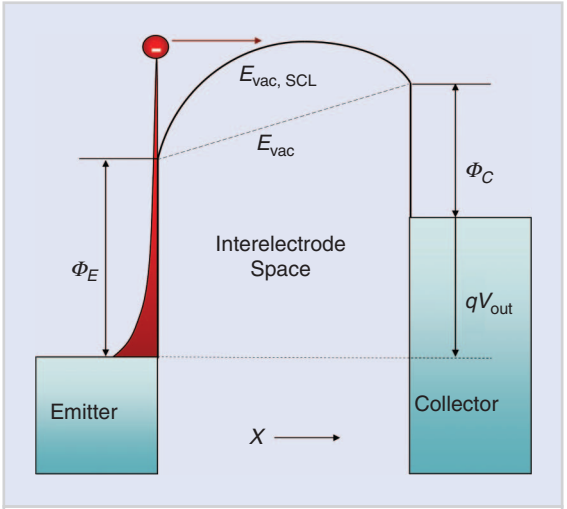

FIGURE 2 The energy diagram of a vacuum TEC: ϕ_E is the emitter workfunction, ϕ_C is the collector workfunction, V_{out} is the output voltage of the TEC, and q is the elementary charge. The red area represents the thermal population of electrons. E_{vac}, SCL is the motive inside the interelectrode space in the space-charge-limited (SCL) regime and E_{vac} is the motive when the space-charge effect is eliminated.

Because of the exponential dependence of TEC current on temperature, small increases in temperature can lead to substantial improvements in efficiency. Thermionic converters have the potential to operate at exceedingly high temperatures—on par with temperatures generated by the burning of fossil fuels. On the other hand, turbines require operation at much lower temperatures to preserve structural integrity, due to the presence of mechanical stress and vigorous conditions such as hot fluids and chemical products resulting from the combustion process. Therefore, the maximum attainable efficiency is considerably higher in thermionic converters and closer to the Carnot efficiency. For instance, coal is one of the most dominant fuel sources—responsible for the generation of a substantial portion of the world's electricity—and burns at about 1,500 °C, whereas turbines usually operate significantly below this point (about 700 °C) [4]. Consequently, TECs exhibit inherent advantages over their turboelectric counterparts due to the lack of moving parts in their structure. This feature endows them with potential advantages in cost, reliability, and weight.

FACTORS AFFECTING EFFICIENCY

The two most significant factors affecting the efficiency of TECs are the workfunctions of the electrodes and the space-charge effect in the interelectrode region. Conceptually, the workfunction of the emitter can be considered the energy barrier to the thermal evaporation of electrons into free space, as seen in the TEC energy diagram in Figure 2. According to the Richardson–Dushman equation described, the number of electrons that are able to surmount this barrier is proportional to $\exp(-\phi_E / k_B T_E)$ for a given electrode size and duration of time, where T_E is the temperature of the emitter. The difference between

the emitter and collector workfunctions, $\phi_E - \phi_C$, can be considered a measure of the open-circuit voltage.

Ideally, the collector workfunction should be as small as possible, and, as a rule of thumb, the emitter workfunction should be about 1 eV higher than the collector workfunction to maximize efficiency [3]. So far, no suitable metals have been found that combine stability at high temperatures and sufficiently low workfunctions for near-optimal performance. To maintain a stable, low workfunction, the electrodes are often immersed in alkali metal vapor, due to the low workfunction of alkali metals.

The electrons ejected from the hot emitter have a finite speed and thus require a finite amount of time to travel to the collector. The electrons occupy the interelectrode space during this time, forming a cloud of negative space charge. This gives rise to an electric field, which repels newly ejected electrons, and only those with sufficient kinetic energy to overcome this repulsion may reach the collector. This effect can be seen in the energy diagrams in Figures 2 and 3. The regimes of operation of the TECs are also illustrated in Figure 3. In vapor TECs, this electric field is reduced, to a degree, by the positive ions of the alkali metal present in the vapor. However, some electrons collide with these vapor atoms elastically and inelastically, which may cause them to return to the emitter, adding to the undesirable reverse current [3].

REDUCING THE EMITTER WORKFUNCTION

The emitter materials of TECs have traditionally been chosen from refractory metals with workfunctions on the order of 4–5 eV. This leads to the need for very elevated temperatures to achieve reasonable levels of emission current and output power. These high temperatures lead to implementation difficulties and increased losses due to the spread of heat to the surroundings and incandescence from the hot emitter. Therefore, the metals were typically coated with low-workfunction materials, which were not stable.

ALKALI METAL INTERCALATION

One way to circumvent this issue in nanomaterials is through the inclusion of alkali metals into the small spaces between atomic/molecular layers of the host, also known as intercalation. This process requires energy to increase the distance between the host layers against the van der Waals force. This energy can be supplied by means of external heat as well as exothermic interaction due to charge transfer between the guest molecules and the host. Two common examples include stage-1 (C_8K) or stage-2 ($C_{24}K$) K/CNT, where the stage number refers to the number of potassium atoms between the carbon layers, C is carbon, K is potassium, and CNT stands for carbon nanotube.

Intercalated nanomaterial emitters have potential advantages over refractory metal emitters with alkali metals deposited on the surface. The latter are relatively unstable and tend to continuously evaporate or change their morphology on the surface, as they have low melting and boiling points. Therefore, a reservoir containing alkali metals is usually necessary to have the TEC operate consistently [3]. Intercalated nanomaterials, on the other hand, not only substantially reduce the workfunction of the host material but may also exhibit higher temperature stabilities [5].

Various types of carbon have been studied as thermionic emitters [6]. Therefore, developing methods of reducing their workfunctions is highly desirable. Pristine carbon nanofibers and nanotubes have workfunctions in the range of 4–5 eV, similar to that of polycrystalline graphite [7]. The workfunction of a CNT depends on several factors, such as its chirality, diameter, and surface oxidation condition [5]. However, by optimization of these parameters, the workfunction can be only marginally reduced. It is also possible to modify the workfunction of CNTs using adsorbates. However, because of weak intermolecular attraction, the stability of the resulting structure is not adequate for the high temperatures required by TECs. On the other hand, it is possible to significantly reduce the workfunction of CNTs by alkali metal intercalation. It has been observed that intercalates of potassium or cesium with single-walled CNTs exhibit workfunctions of 3.3 and 2.4 eV, respectively [8], [9]. Intercalates have also been formed

> Thermionic converters have the potential to operate at exceedingly high temperatures—on par with temperatures generated by the burning of fossil fuels.

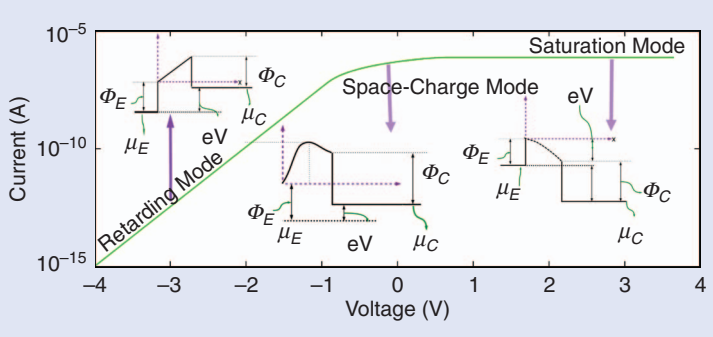

FIGURE 3 The current–voltage characteristics of a TEC under different operating conditions and the corresponding energy band diagrams. The three main regimes of operation are the retarding mode, the space-charge mode, and the saturation mode. μ_E and μ_C represent the electrochemical potentials of the emitter and collector, respectively, and V is the output voltage.

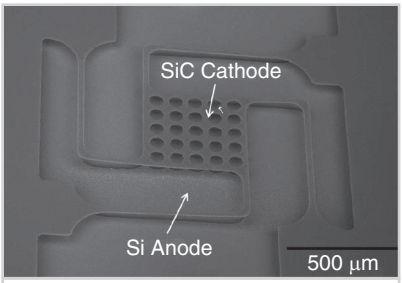

FIGURE 4 A scanning electron micrograph of a microfabricated TEC with SiC as the emitter and a silicon substrate as the collector, with an etched gap of ~50 μm. (Reprinted with permission from [18], © 2012, IEEE.)

from stoichiometric reactions of molten potassium with various types of graphitic carbon nanofibers. Stage-1 K with herringbone graphitic carbon nanofiber (GCNF) showed a reduced workfunction of about 2.2 eV and stability up to 1,300 K [5]. Other work has shown that potassium intercalated CNTs can be stable up to 820 K [9].

OTHER APPROACHES

Another interesting method to reduce the workfunction is by means of nanostructure geometry engineering. By coating the surface of the emitter with a thin metal layer with periodic ridges, a series of quantum wells are formed [10]. By imposing the resulting additional boundary conditions on the electron wave function at the surface, it is possible to introduce forbidden states. Electrons are banned from filling these states and, therefore, occupy higher energy levels, raising the chemical potential and correspondingly reducing the workfunction.

Advances in stable low-workfunction materials have prompted investigations into their use as emitters in vacuum TECs. N-type diamond thin films, doped with nitrogen, have exhibited effective workfunctions of less than 2 eV. Low-electron-affinity aluminum gallium nitride (AlGaN) thin films also show promise as TEC emitter materials, although band bending due to surface states has pushed the workfunction to above 2.3 eV in practice [11].

The energy barrier that electrons see before thermionic emission can be effectively reduced in a gas discharge environment. The local electric field at the emitter can be modified because of the presence of ions exiting the discharge region. Go et al. theoretically studied the influence of ions from a gas discharge on thermionic emission of electrons. Their analysis reveals that the presence of ions can significantly increase the thermionic emission current, with more tangible effects in the case of stationary ion charges [12].

MITIGATING THE SPACE-CHARGE EFFECT

As mentioned previously, the cloud of electrons between the two electrodes creates a potential barrier for the electrons ejected from the emitter. This effect is exacerbated as the current density increases, as the distance between the electrodes increases, and as the average electron speed decreases [3]. Several solutions have been proposed to mitigate the space-charge effect.

APPLIED ELECTRIC AND MAGNETIC FIELDS

One way to decrease or eliminate the potential barrier created by the negative space-charge cloud is to apply an electric or magnetic field to the electrode gap via an auxiliary electrode. This effectively allows one to engineer the electron distribution in space to minimize the space-charge barrier. The first of the two most-prominent triode TEC designs is the magnetic triode, in which crossed electric and magnetic fields steer electrons toward a collector lying on the same plane as the emitter. The other configuration is the electrostatic triode, in which a grid is placed between the electrodes to change the electric potential landscape to accelerate electrons.

In vapor TECs, the negative space-charge cloud is meant to be compensated for with positive ions. These ions can be produced by thermionic emission from the surface of the emitter or by collision of emitted electrons with vapor atoms. However, the ionization potential of these alkali metals is usually around 4 eV, and most of the thermionically emitted electrons do not have sufficient kinetic energy to ionize these atoms. Therefore, the ions are usually introduced by some other means, such as an arc discharge between the emitter and an auxiliary electrode, where the electric field is strongest. This results in a significant loss in the output power of the TEC.

More recently, advanced vapor TECs have been proposed that use an auxiliary grid electrode in combination with a longitudinal magnetic field. These TECs theoretically reduce or eliminate the space-charge effect [4]. Two device configurations have been proposed by Moyzhes et al. [13]. In the first one, the hot electrons needed for ionizing the alkali metals are trapped in a potential well and separated from the thermionic current. In the second one, the alkali metal vapor atoms are ionized directly on the gate electrode.

NEGATIVE ELECTRON AFFINITY MATERIALS

It is possible to lower the electrons' potential energy level just outside the emitter surface—the vacuum level of the emitter—to fall below its conduction band. This class of emitters is known as negative-electron-affinity (NEA) materials. Several surface orientations of diamond exhibit NEA behavior when terminated by hydrogen. This property, along with the low thermionic barrier in doped diamond, makes it an attractive candidate for thermionic emission. This mechanism opens a route to alleviate the space-charge effects. When electrons emitted from the conduction band reach the vacuum level, their kinetic energy will noticeably increase, since the vacuum level rests at a lower energy than the conduction band. Therefore, NEA can effectively reduce the number of slower electrons, which spend the most time in the interelectrode region and thus contribute most significantly to the space-charge barrier [14]. NEA materials may also present an effectively lower barrier to electron emission due to quantum-mechanical tunneling.

REDUCING THE INTERELECTRODE SPACING

Decreasing the distance between the electrodes is a straightforward approach to mitigate the space-charge effect, although energy loss via radiative heat transfer between the electrodes may become significant, especially as the electrode spacing approaches the submicrometer range. At large gaps, heat is transferred between the electrodes primarily via propagating

electromagnetic waves, following the Stefan–Boltzmann law. Evanescent electromagnetic waves, which decay exponentially away from the electrode surface, i.e., surface plasmon polaritons, are also excited by incident radiation. When the electrode gap shrinks to a distance on the order of the characteristic wavelength of blackbody radiation, these waves begin to couple to each other in an effect sometimes called *photon tunneling* [15]. In TECs with this small of an electrode gap, this form of radiative heat transfer becomes rapidly dominant and severely limits the efficiency.

Lee et al. [16] have combined the equations for SCL thermionic current with far-field and near-field heat-transfer calculations to determine the optimal emitter–collector gap for a TEC. For near-ideal emitter and collector materials, the optimal gap for peak efficiency was found to lie between 0.5 and 1 μm, depending on emitter temperature. At electrode gaps of this size or smaller, the space-charge effect essentially becomes insignificant. Fortunately, devices with such electrode gaps can be readily fabricated using current microelectromechanical systems fabrication technologies. At least one U.S. patent has been filed for such a device [17]. Thermionic devices with gaps as small as 1.7 μm have been fabricated with silicon carbide (SiC) emitters and silicon collectors using standard surface micromachining techniques, as seen in Figure 4 [18]. Thermionic conversion was successfully demonstrated by resistively heating the suspended SiC electrode up to 2,000 K (in the 50-μm-gap device), and no undesired contact was made between the electrodes. However, the conversion efficiency was still severely limited by the high workfunction of SiC.

The previous discussion concerning the efficiency of TECs with submicron electrode gaps only dealt with thermionic emission of electrons. In theory, another peak in efficiency could potentially occur at an electrode gap on the order of a few nanometers, when electron tunneling becomes significant. The characteristics of nanoscale-gap TECs based on cesium iodide-coated graphite have been studied based on electron tunneling and radiative-heat-transfer calculations [19]. The electric current was found to be drastically higher but with a comparably severe increase in evanescent-wave radiative heat transfer. For an electrode gap of this size, the electrode materials would need to be carefully chosen for their optical properties to minimize evanescent-wave coupling [20].

Another significant challenge lies in the fabrication of devices with such small gaps. Electrodes with a vacuum gap smaller than 5 nm and area larger than 7 mm^2 have been successfully fabricated using an electroplated copper/silver/titanium/silicon (Cu/Ag/Ti/Si) structure, where the layers separate as a result of differing thermal expansion coefficients and controlled adhesion properties [21]. A different proposed solution is to place dielectric nanowires between planar electrodes to obtain a fixed, nanometer-scale gap [22].

LIGHT-INDUCED THERMIONIC EMISSION

The energy of photons can be exploited to heat the emitter material to sufficiently high temperatures and thus have light-induced thermionic emission (LITE). Naturally, an abundant and free source of light is the sun. A solar thermionic generator is a special case of a TEC, namely, a light-induced TEC (LITEC).

In a single-junction photovoltaic cell, photon absorption is limited to the bandgap energy, which creates an inherent limitation on efficiency. Energy from incident photons exceeding the bandgap will be lost as heat, while photons with subbandgap energies are simply not absorbed, severely restricting the quantum efficiency. This effect is mitigated in multijunction photovoltaic cells, which absorb photons at several discrete energies. A TEC relies on heating, which does not directly depend on this bandgap energy, and, theoretically, the entire absorbed portion of the spectrum of the incident light maybe used. Moreover, the structure of a LITEC is, in principle, relatively simple and robust and does not require high-quality semiconductors.

LITECs are not well established in the clean-energy industry yet due to several practical issues in their implementation. The intricate connection between thermal and electrical conductivity is primarily responsible. An excellent electrical conductivity is necessary in a TEC, but this normally comes with high thermal conductivity, which leads to substantial heat loss to the surroundings. Consequently, extremely high incident powers and large, elaborate light-focusing contraptions are required to reach the optical intensities required to achieve the desired temperature.

Heating the emitter to temperatures of >1,500 K remains challenging, even with the most advanced technology. Of note is NASA's High Power Advanced Low Mass solar thermionic system, which features extremely large, complex light-collection and -focusing structures that are often several meters in diameter [23]. An example solar thermionic device developed by NASA is shown in Figure 5.

In light of the difficulties associated with solar heating of the emitter, most tests performed on LITEC devices have used alternative methods such as electrical heating. Under carefully designed experimental conditions, efficiencies as high as 11% have been achieved in this manner [23].

Light-harvesting TECs convert solar radiation into thermal energy, producing electricity via a heat engine, whereas photovoltaic cells use the quantum nature of light to excite electrons to higher energy bands. The processes could potentially be combined through thermally enhanced photoemission or photon-enhanced thermionic emission [24]–[27]. The situation may further be improved by coating the surface with metal nanoparticles,

FIGURE 5 The NASA solar TEC prototype consists of a 3-m-diameter concentrating mirror with dual-axis tracking. (Reprinted with permission from [23]. © 2006, AIP Publishing LLC.)

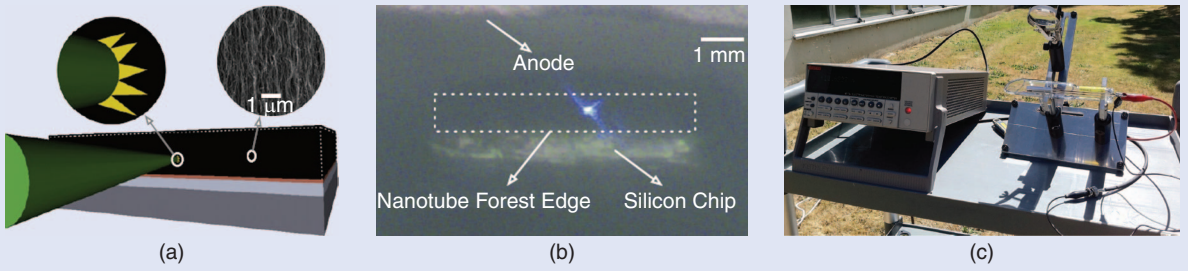

FIGURE 6 (a) A schematic diagram of a CNT-based LITE device. As the intensity of the incident beam surpasses a threshold value, an incandescent spot is observed. The inset depicts a scanning electron micrograph of the sidewall of the CNT forest. (b) A charge-coupled device camera was used to capture a photo of the hot spot. Note the size of this spot with respect to the forest edge, showing the localized nature of heating, while the rest of the forest remains cool. (Reprinted from [29] with permission from Elsevier.) (c) A CNT-based solar thermionic emitter in a portable sealed glass vacuum chamber [30]. A small lens can focus enough solar power to reach thermionic emission temperatures. Compare the simplicity of this device with that of the apparatus shown in Figure 5. (Used in accordance with the Creative Commons Attribution 3.0 Unported License.)

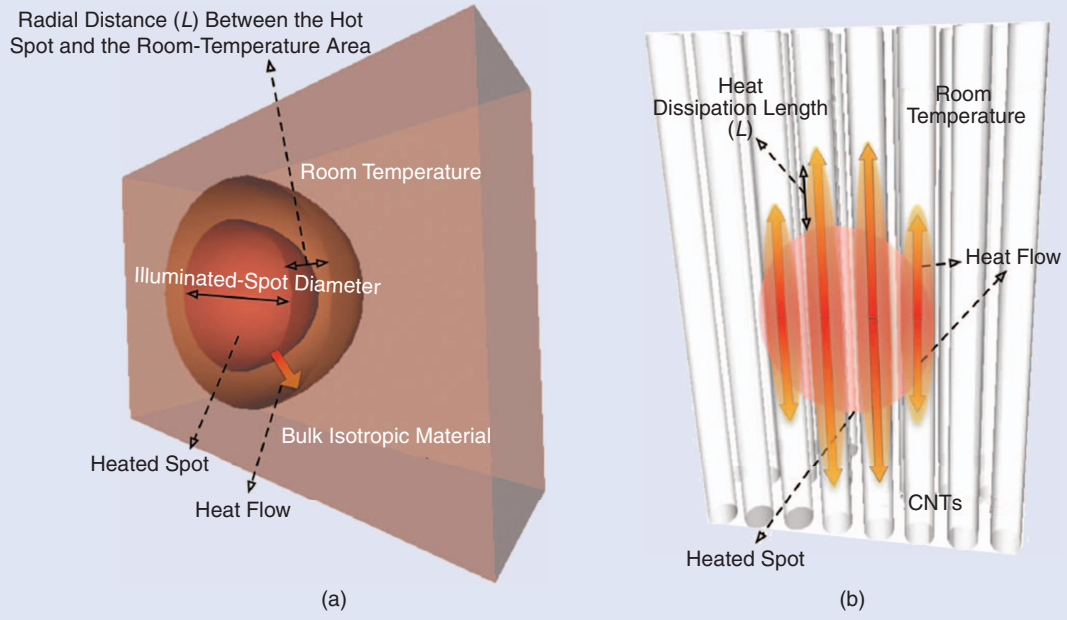

FIGURE 7 The heat transport in (a) a bulk emitter in contrast to (b) a CNT forest. In a bulk electrode, heat transfers to a much larger area than the source region because of high thermal conductivity. However, CNTs are highly anisotropic, and most of the heat flows only along the axial direction. Together with the rapid drop in the thermal conductivity of nanotubes with temperature, this leads to the heat-trap effect. Therefore, the issue of heat spread is substantially mitigated [30]. (Used in accordance with the Creative Commons Attribution 3.0 Unported License.)

which has been shown to enhance light absorption via a plasmonic process by increasing the effective optical path length inside the active layer, therefore increasing overall absorption [28].

CNT-BASED LITECS

Nanomaterials exhibit intriguing thermal and mechanical properties and could potentially circumvent some of the challenges associated with traditional TECs. Several salient features, such as high surface area, high mechanical strength, and resilience to high temperatures, make them promising candidates for thermionic applications. CNTs are particularly interesting in this context because of additional desirable characteristics, such as their quasi-one-dimensionality and high absorptivity over a broad spectral range. Electrons are confined in the transverse directions, limiting the energy states into which they can scatter, thus increasing the mean free path and conductivity.

Interestingly, CNTs have recently been shown to overcome the fundamental challenge of the spread of light-induced heat in emitters. When an array of multiwalled CNTs (a so-called CNT forest) is illuminated by a sufficiently focused low-power beam of light, a heat-trap effect is observed (Figure 6). This highly localized heating mechanism allows the illuminated spot to be heated to thermionic emission temperatures (>2,000 K), without significantly heating the surroundings [29]. This effect

was attributed to two main factors, including a rapid drop in the thermal conductivity versus temperature in CNTs, as opposed to a less-rapid drop in bulk materials, as well as the quasi-one-dimensional nature of heat transport in CNTs as contrasted with isotropic bulk materials (Figure 7). By mitigating the heat spread to the surroundings due to the localized nature of the heat spot, this effect eliminates a major loss mechanism in thermionic conversion.

Among other parameters such as the density and uniformity of the CNT forest, the threshold incident power required to induce the heat-trap condition depends primarily on the area of the illuminated spot. For an incident light beam diameter of several hundred micrometers, the threshold intensity is on the order of 50 W/cm^2 [29]. Assuming that photons of different energies of the solar spectrum all contribute to heating, the average sunlight intensity on the surface of the earth, once focused with a handheld glass lens, will suffice to thermionically emit electrons from CNTs based on this effect (Figure 6).

Accordingly, a solar LITEC has been demonstrated based on this phenomenon [30]. The efficiency of the first device at peak power was low (10^{-6}%). However, this low efficiency is not a fundamental limit (as shown by NASA's LITEC devices [23]), and major improvements are possible. Moreover, even this early prototype exhibited a short-circuit current density and peak power density comparable to those of state-of-the-art photovoltaics. This is a testament to some of the inherent advantages of LITECs, which are understood to enable higher power densities than photovoltaic devices. As can be seen in Figure 8, the open-circuit voltage of these devices can also be appreciably higher than that of most photovoltaic devices.

The most conspicuous improvements will arise from a reduction of the workfunction of the CNTs. Although the issue of heat transfer to the surroundings is minimized, major energy loss takes place through incandescence from the hot spot. By reducing the workfunction of the CNTs and thus operating at lower temperatures (without sacrificing the electron emission current), the energy loss due to radiation of heat can be substantially reduced. As the theoretical prediction of Figure 9 shows, the efficiency can be enhanced by several orders of magnitude if the workfunction of CNTs is reduced by about 2 eV.

Further improvements can be attained by reducing the space-charge effect through the optimal design of the device as well as by using aspherical lenses and more-sophisticated optics to reduce chromatic aberrations and allow for the better focusing of sunlight.

THERMOELECTRIC CONVERSION

Thermoelectric converters have much in common with thermionic converters, but the interelectrode vacuum between the emitter and collector is replaced by a solid material in thermoelectric converters. In 1821, Seebeck discovered that if metal A is joined at both ends by metal B, and a temperature difference exists between the two junctions of dissimilar metals, an induced potential difference will appear across the two free ends of metal B (held at the same temperature), thus forming a thermocouple. The differential Seebeck coefficient, α_{AB}, is the ratio of the induced voltage to the temperature difference, $V/\Delta T$. By convention, α is positive if the electromotive force tends to drive an electric current through conductor A from the hot junction to the cold junction. Seebeck coefficients are typically on the order of a few μV/K for metals and hundreds of μV/K for semiconductors.

Shortly after, in 1834, Peltier discovered the opposite effect, whereby passing an electric current through a thermocouple results in a small heating or cooling at the junctions, depending on the direction of current. In practice, it is difficult to demonstrate the Peltier effect on metallic thermocouples due to the inevitable presence of Joule heating. The differential Peltier coefficient, Π_{AB}, is the ratio of the inward (or outward) heat flux to the current through the junction, Q/I. By convention, Π is positive if the junction through which the current enters conductor A is heated and if the junction through which current leaves A is cooled. Figure 10 shows a schematic of the Seebeck and Peltier effects using a p-n junction.

In 1855, Thomson, also known as Lord Kelvin, realized that the Seebeck and Peltier effects are dependent on one another as seen by $\Pi_{AB} = \alpha_{AB} T$. He also realized that there is reversible heating or cooling in homogeneous conductors when there is both a flow of current and a temperature gradient. The Thomson coefficient (τ) is the rate of heating per unit

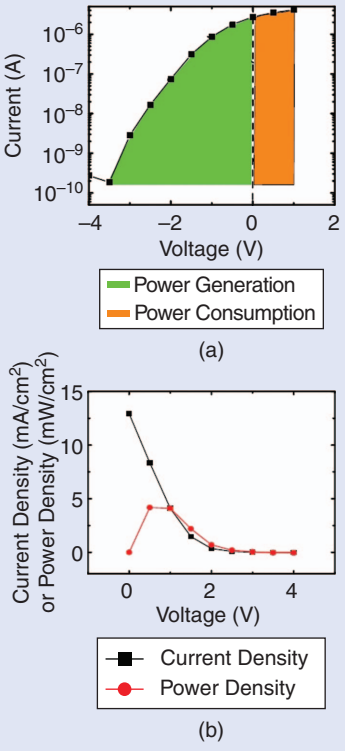

FIGURE 8 (a) The current–voltage characteristics of a CNT-based solar LITEC device. (b) The corresponding generated current and power densities [30]. (Used in accordance with the Creative Commons Attribution 3.0 Unported License.)

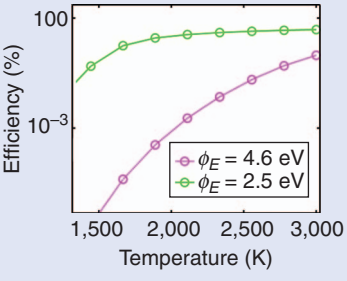

FIGURE 9 The simulated values of the efficiency as a function of temperature for CNT-based LITECs with different workfunction values. Higher efficiencies can be achieved at lower temperatures as the workfunction of the material is reduced. (This model includes space-charge effects but neglects back-emission from the collector to the emitter.)

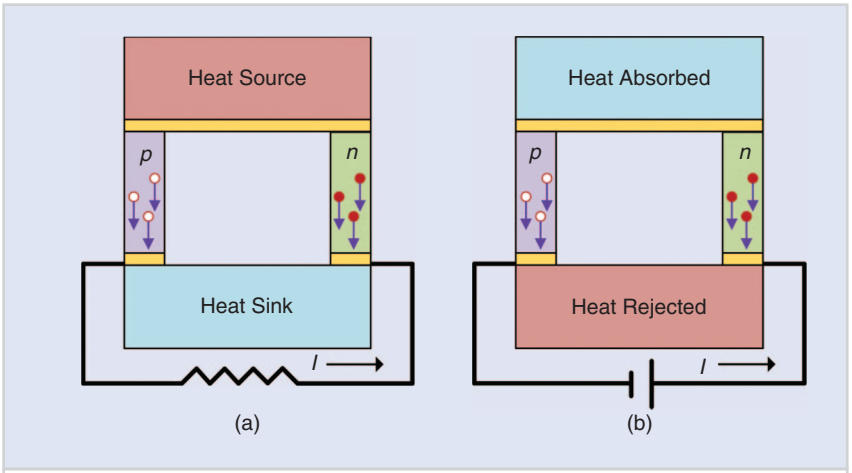

FIGURE 10 A schematic diagram of (a) a Seebeck power-generation device and (b) a Peltier refrigeration device made from a p-n junction.

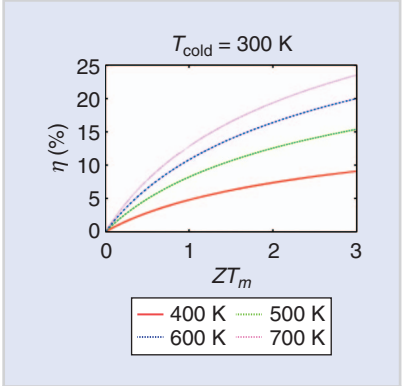

FIGURE 11 A plot of the energy conversion efficiency versus dimensionless figure of merit for a heat sink at 300 K and a heat source at varying hot-side temperatures.

length per unit temperature resulting from passing a unit of current along a conductor where there is a temperature gradient.

With the advent of sensor and actuator technology, the need for regenerative and decentralized small power sources has risen. Some of the advantages of the Seebeck effect are its quietness, compactness, and robustness. For example, NASA's Voyager and Cassini missions already use this effect in their radioisotope thermoelectric generators [31]. Another application for the Seebeck effect could be in the conversion of automotive waste engine or radiator heat into useful electric energy.

Unfortunately, the efficiency (η) of thermoelectric generators based on bulk materials is still intrinsically low. Nanostructured thermoelectric materials have the potential to have efficiencies greater than their bulk counterparts due to reasons that will be discussed. Generators based on these structures offer the ability to convert waste heat into microwatts to milliwatts of usable electrical energy, which, for example, is sufficient to power a microcircuit.

FIGURE OF MERIT

The thermoelectric effects themselves are thermodynamically reversible; however, practical devices always contain some form of electrical resistance and thermal conduction losses. The performance of a thermoelectric device can be quantified as a function of the Seebeck coefficient and the electrical and thermal conductances of the two connected materials. There needs to be a material with high electrical conductivity to allow for easy passage of charge and low thermal conductivity to enable the device to operate under high temperature gradients. Therefore, the dimensionless figure of merit for a single thermoelectric material is defined as

$$ZT = \frac{\alpha^2 \sigma T}{k},$$

where α is the Seebeck coefficient, σ is the electrical conductivity, T is the temperature in Kelvin, and k is the thermal conductivity. For energy conversion applications, it is highly desirable to maximize ZT. The efficiency of thermoelectric power generation (Seebeck effect) is defined as the ratio of energy supplied to the load over the heat energy input, which can be shown to be equal to [32]

$$\eta = \frac{T_H - T_C}{T_H} \frac{\sqrt{1+ZT_{\text{avg}}} - 1}{\sqrt{1+ZT_{\text{avg}}} + \frac{T_C}{T_H}} = \eta_{\text{Carnot}} \frac{\sqrt{1+ZT_{\text{avg}}} - 1}{\sqrt{1+ZT_{\text{avg}}} + \frac{T_C}{T_H}},$$

where T_H and T_C are the hot- and cold-side temperatures. It can be seen that by increasing ZT, the device efficiency can approach the Carnot efficiency. In this case, as the temperature gradient is increased, the device efficiency is also increased. Figure 11 shows a plot of efficiency versus ZT for increasing values of temperature differences.

BULK MATERIAL LIMITATIONS

In classical bulk thermoelectric materials, α, σ, and k all depend on one another, which impedes the optimization of Z. The numerator of ZT is mostly determined by charge carriers and the denominator by the conduction of heat by acoustic phonons. A higher density of electrons raises σ but lowers α (which is undesirable). Longer electrons mean free paths improve σ without decreasing α, but this is usually achieved in crystals with a low density of defects, meaning longer phonon mean free paths and a higher k (undesirable).

Historically, metals were the only conductors properly known, and, unfortunately, all metals showed values of ZT much less than one for all temperatures. By using the free electron gas model and varying the electron density, n, Ioffe showed that there exists a maximum in the Z versus n curve at $n = 10^{19}$ cm^{-3}, which can be achieved by doping semiconductors with impurities [33].

The power factor ($\alpha^2\sigma$), or the numerator of the figure of merit, is maximized in narrow-bandgap ($E_g \approx 10\, k_B T$) doped semiconducting materials [34]. The bandgap must also be sufficiently large to minimize the minority carrier contributions to the overall Seebeck coefficient [35]. High-mobility carriers ($\mu \approx 2{,}000$ cm^2/Vs) are desirable to give the highest electrical conductivity for a given carrier concentration.

The thermal conductivity k is a measure of the heat transfer through a material by electrons (k_{el}) and by phonons (k_{ph}),

where both should be suppressed. According to the Wiedemann–Franz Law, the electronic portion of thermal conductivity is directly proportional to electrical conductivity. Therefore, there is a tradeoff in optimizing ZT. Reducing k_{ph} is also an important task, since phonon heat flow from the hot junction to the cold junction will reduce the temperature gradient. This problem is further complicated in nanoscale devices. A short discussion on minimizing k_{ph} will follow.

EXISTING THERMOELECTRIC MATERIALS

Ongoing research in this field has been focused on either raising the efficiency of thermoelectric devices (increasing ZT) or expanding the useful operating temperature range. Figure 12 shows ZT as a function of temperature for several researched bulk thermoelectric materials. It is important to note that a thermoelectric device operates at its maximum ZT at a specific temperature. The current commercially available thermoelectric devices are split into three categories, depending on the temperature range. Bismuth (Bi) alloys with antimony (Sb), tellurium (Te), and selenium (Se) are low temperature (up to 450 K) and are typically used in Peltier refrigeration. Lead telluride (PbTe) devices are intermediate temperature (up to 850 K). Silicon germanium (SiGe) alloys are high temperature (up to 1,300 K) [36]. However, despite decades of research on bulk materials, the practical value of ZT has yet to surpass approximately one.

MINIMIZING PHONON THERMAL CONDUCTIVITY

Recently, efforts have been focused on improving the figure of merit by minimizing k_{ph}. Phonon glass-electron crystals (PGECs) are a promising type of material capable of conducting heat like an amorphous glass and conducting electricity like an electronic crystal [38]. In other words, these materials have low lattice thermal conductivities and high electrical conductivities. Clathrates (Figure 13) are PGECs with a cage-like structure usually made up of silicon or germanium atoms. Within the cage, loosely bound alkali guest atoms rattle around and give rise to intense phonon scattering, thereby reducing the phonon thermal conductivity of the material. Similar to clathrates, skutterudites are another type of PGEC. Skutterudites (Figure 13) are binary compounds with the atomic composition of MX_3, whereby M atoms are Group 9 transition metal atoms situated at the corners of the cage, and X atoms are Group 15 nonmetals. Rare-earth atoms fill the voids and rattle around inside the cage structure.

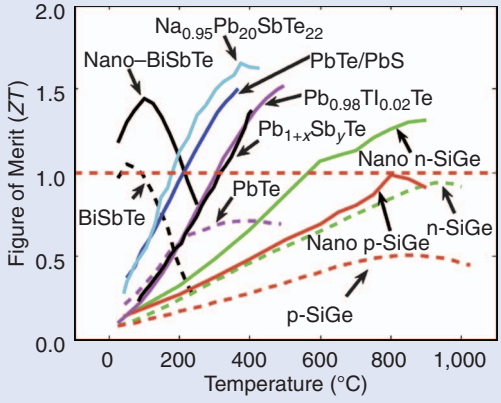

FIGURE 12 The performances of some of the well-established thermoelectric materials as a function of temperature. (Reproduced from [37] with permission from The Royal Society of Chemistry.)

REDUCED DIMENSIONALITY

Although thermoelectric effects were first used in metals, semiconductors have been more practically used since the 1950s because of their stronger manifestation of these effects. The promise of nanotechnology and nanostructured thermoelectric materials arises from the dimensionality of the system being a new working parameter. Low-dimensional structures such as quantum wells [two-dimensional (2-D)], quantum wires [one dimensional (1-D)], and quantum dots [zero-dimensional (0-D)] are thus believed to represent

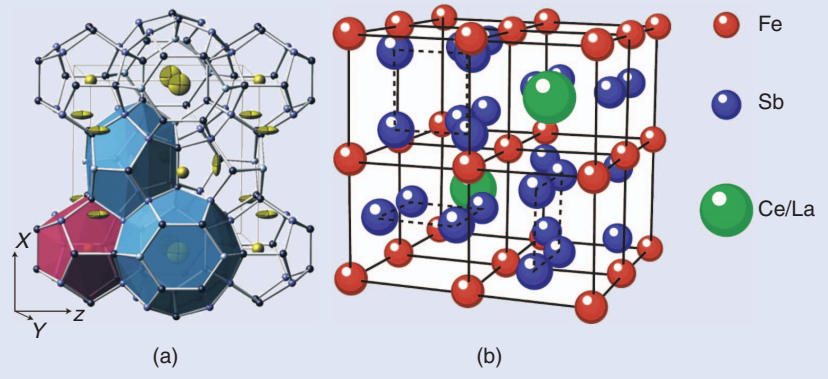

FIGURE 13 (a) A Ba8Ga16Ge30 clathrate structure, where Ga and Ge (blue) host atoms surround the Ba (yellow) guest atoms. (b) A Skutterudite structure, where Fe and Sb (red and blue) atoms surround the Ce or La (green) guest atoms. [(a) reprinted with permission from Macmillan Publishers Ltd. [39], © 2008. (b) reprinted with permission from Macmillan Publishers Ltd. [40], © 2008.]

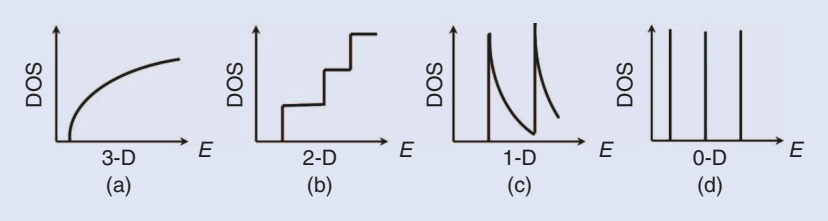

FIGURE 14 Electronic DOSs $g(E)$ as a function of carrier energy (E): (a) a bulk semiconductor, (b) a quantum well, (c) a quantum wire, and (d) a quantum dot. (Reprinted with permission from [42].)

another approach for improving the figure of merit through reducing the interdependence of the relevant coefficients—the Seebeck coefficient and the electric and thermal conductivities. Nanostructures provide a means for tuning the ZT through quantum confinement, modulation doping, and the increased influence of interfaces and surfaces [41]. Theoretical and experimental measurements on nanostructures over the past decade have shown steadily increasing values of ZT.

In the domain of low-dimensional solids, we define the sample length scale, d, as follows: in 2-D structures such as quantum wells, d is the well width; in 1-D or 0-D structures such as quantum wires or dots, d is the diameter. This length scale can be taken advantage of with two important realizations. First, in the diffusive transport regime, the electrical conductivity, σ, is determined by the electron mean free path (l_e) and the phonon thermal conductivity, k_{ph}, is determined by the phonon mean free path (l_{ph}). Nanostructures should be constructed with length scales that limit l_{ph} but not l_e [34]. Doing so can potentially reduce the thermal conductivity without decreasing the electrical conductivity.

Second, size-quantization effects can increase the Seebeck coefficient without affecting the charge carrier density and electrical conductivity. Since the Seebeck coefficient is a function of the energy derivative of the electron density of states (DOS), it is enhanced when the DOS is a sharply peaked function of energy, as is the case in lower dimensional materials as depicted in Figure 14. For these two realizations to hold true, the system must be free from disorder as much as possible so that the band structure model holds true. In particular, for small values of d, there is a high possibility that defects can localize the electron wavefunction to one portion of the device and impede electron transport.

A low thermal conductivity is highly desirable for a highly efficient thermoelectric device. Through a series of experiments, thermal conductivity has been shown to decrease with decreased system dimensionality. For example, $FeSb_2$ nanostructures have shown a thermal conductivity reduction by three orders of magnitude compared to the single-crystal material [43].

Thermal conductivity has been seen to increase as the finite size along the free direction of the system increases. In 1-D systems such as single-walled CNTs, for example, k increases with a power-law dependence [44]. In 2-D systems, k grows logarithmically [45]. However, k does not diverge in 3-D systems.

Scattering mechanisms can be classified as either intrinsic or extrinsic. Umklapp scattering, where phonon crystal momentum is not conserved, is a type of phonon–phonon intrinsic scattering. This dominates over normal scattering, where phonon momentum is conserved, in bulk 3-D solids at temperatures above 1/10th of the Debye temperature of the material. Thermal conductivity has also been shown to be limited by extrinsic scattering, or phonon-boundary scattering, in single-walled CNTs with d less than l_{ph} [46]. Through molecular dynamics simulations, the increased surface scattering in fractal-like nanoporous silicon has shown large reductions in thermal conductivity relative to bulk [47].

Various groups have fabricated silicon nanowires with diameters in the tens of nanometers for thermoelectric applications [48], [49]. Nanowire diameter, doping, and roughness were all controlled. While the Seebeck coefficient and electrical conductivity were unchanged compared to bulk silicon, the silicon nanowires showed a 100-fold decrease in thermal conductivity. This was explained due to the device length scale d being less than the phonon mean free path (~300 nm at 300 K), but larger than the electron mean free path (~110 nm at 300 K). ZT was thus enhanced by efficient phonon scattering to 0.6 at room temperature.

Low-dimensional nanostructures have thus exhibited the potential to improve the thermoelectric figure of merit relative to their bulk 3-D counterparts. Nanostructured materials offer the advantage of weakening the interdependence of the three thermoelectric parameters—the Seebeck coefficient, the electrical conductivity, and the thermal conductivity. However, despite decades of ongoing research, the world record ZT remains at 2.2 at 915 K [50]. Thermoelectric energy conversion efficiency is still limited by parasitic thermal backflow in the legs of thermocouples or, in other words, a phonon thermal conductivity that is still too high. For this reason, thermionic energy conversion has potential advantages as the vacuum gap blocks phonons while allowing electron transmission. However, recall the heat-trap effect in CNT arrays, where extremely high temperature gradients are maintained within this otherwise-conducting material [29]. This unusual phenomenon, enabled by nanostructures, may thus open up avenues for potentially high-performance thermoelectric devices for converting light to electricity. Perhaps it will also be possible to achieve the heat-trap condition without illumination, and thus create new thermoelectric devices for the direct conversion of heat to electricity.

SUMMARY

Thermionic and thermoelectric energy converters are highly promising candidates for clean energy generation devices. However, the widespread application of thermionics has been limited because of the space-charge effect and the need for electrode materials with low workfunctions and high thermal stability. The pursuit of high-efficiency thermoelectric devices has been plagued by the difficulty of finding low-thermal-conductivity materials that maintain high thermopowers. Nanostructured materials, with the new opportunities that they provide for overcoming some of the existing challenges, represent some of the most promising methods toward harvesting solar and waste heat energy.

ACKNOWLEDGMENTS

We would like to thank the University of British Columbia, the Natural Sciences and Engineering Research Council of Canada, the Canada Foundation for Innovation, the British Columbia Knowledge Development Fund, the BCFRST Foundation, and the British Columbia Innovation Council for the financial support of our work on electron emission and energy conversion. Harrison D.E. Fan and Andrew T. Koch contributed equally to this work.

ABOUT THE AUTHORS

Amir H. Khoshaman (akhosham@ece.ubc.ca) is with the Department of Electrical and Computer Engineering, University of British Columbia, Canada.

Harrison D.E. Fan is with the Department of Electrical and Computer Engineering, University of British Columbia, Canada.

Andrew T. Koch is with the Department of Electrical and Computer Engineering, University of British Columbia, Canada.

George A. Sawatzky is with the Department of Physics and Astronomy, and the Department of Chemistry, University of British Columbia, Canada.

Alireza Nojeh (anojeh@ece.ubc.ca) is with the Department of Electrical and Computer Engineering, University of British Columbia, Canada.

REFERENCES

[1] A. C. Marshall, "A reformulation of thermionic theory for vacuum diodes," *Surf. Sci.,* vol. 517, no. 1–3, pp. 186–206, Oct. 2002.

[2] N. S. Rasor, "Thermionic energy conversion plasmas," *IEEE Trans. Plasma Sci.*, vol. 19, no. 6, pp. 1191–1208, Dec. 1991.

[3] G. N. Hatsopoulos and E. P. Gyftopoulos, *Thermionic Energy Conversion, Vol. 1.* The MIT Press, 1973.

[4] S. Meir, C. Stephanos, T. H. Geballe, and J. Mannhart, "Highly-efficient thermoelectronic conversion of solar energy and heat into electric power," *J. Renew. Sustain. Energy*, vol. 5, no. 4, p. 043127, Aug. 2013.

[5] J. A. Michel, V. S. Robinson, L. Yang, S. Sambandam, W. Lu, T. Westover, T. S. Fisher, and C. M. Lukehart, "Synthesis and characterization of potassium metal/graphitic carbon nanofiber intercalates," *J. Nanosci. Nanotechmol.*, vol. 8, no. 4, pp. 1942–1950, Apr. 2008.

[6] V. S. Robinson, T. S. Fisher, J. A. Michel, and C. M. Lukehart, "Work function reduction of graphitic nanofibers by potassium intercalation," *Appl. Phys. Lett.*, vol. 87, no. 6, p. 061501, 2005.

[7] P. Liu, Y. Wei, K. Jiang, Q. Sun, X. Zhang, S. Fan, S. Zhang, C. Ning, and J. Deng, "Thermionic emission and work function of multiwalled carbon nanotube yarns," *Phys. Rev. B*, vol. 73, no. 23, June 2006.

[8] S. Suzuki, F. Maeda, Y. Watanabe, and T. Ogino, "Electronic structure of single-walled carbon nanotubes encapsulating potassium," *Phys. Rev. B*, vol. 67, no. 11, p. 115418, Mar. 2003.

[9] T. L. Westover, A. D. Franklin, B. A. Cola, T. S. Fisher, and R. G. Reifenberger, "Photo- and thermionic emission from potassium-intercalated carbon nanotube arrays," *J. Vac. Sci. Technol. B*, vol. 28, no. 2, pp. 423–434, 2010.

[10] A. N. Tavkhelidze, "Nanostructured electrodes for thermionic and thermotunnel devices," *J. Appl. Phys.*, vol. 108, no. 4, p. 044313, Aug. 2010.

[11] A. Shakouri, Z. Bian, R. Singh, Y. Zhang, D. Vashaee, T. E. Humphrey, H. Schmidt, J. M. Zide, G. Zeng, J-H. Bahk, A. C. Gossard, J. E. Bowers, V. Rawat, T. D. Sands, W. Kim, S. Singer, A. Majumdar, P. M. Mayer, R. J. Ram, K. J. Russel, V. Narayanamurti, F. A. M. Koeck, X. Li, J.-S. Park, J. R. Smith, G. L. Bilbro, R. F. Davis, Z. Sitar, and R. J. Nemanich, "Solid-state and vacuum thermionic energy conversion," *MRS Proc.*, vol. 886, no. 1, 2005.

[12] D. B. Go, "Theoretical analysis of ion-enhanced thermionic emission for low-temperature, non-equilibrium gas discharges," *J. Phys. D: Appl. Phys.*, vol. 46, no. 3, p. 035202, Jan. 2013.

[13] B. Y. Moyzhes and T. H. Geballe, "The thermionic energy converter as a topping cycle for more efficient heat engines—New triode designs with a longitudinal magnetic field," *J. Phys. D: Appl. Phys.*, vol. 38, no. 5, pp. 782–786, 2005.

[14] J. R. Smith, G. L. Bilbro, and R. J. Nemanich, "Theory of space charge limited regime of thermionic energy converter with negative electron affinity emitter," *J. Vac. Sci. Technol. B*, vol. 27, no. 3, pp. 1132–1141, 2009.

[15] S. Basu, Z. M. Zhang, and C. J. Fu, "Review of near-field thermal radiation and its application to energy conversion," *Int. J. Energy Res.*, vol. 33, no. 13, pp. 1203–1232, 2009.

[16] J. H. Lee, I. Bargatin, N. A. Melosh, and R. T. Howe, "Optimal emitter-collector gap for thermionic energy converters," *Appl. Phys. Lett.*, vol. 100, no. 17, pp. 173904, 2012.

[17] D. B. King, L. P. Sadwick, and B. R. Wernsman, "Microminiature thermionic converters," U.S. Patent 6 509 669, Jan. 21, 2003.

[18] J. H. Lee, I. Bargatin, T. O. Gwinn, M. Vincent, K. A. Littau, R. Maboudian, Z.-X. Shen, N. A. Melosh, and R. T. Howe, "Microfabricated silicon carbide thermionic energy converter for solar electricity generation," in *Proc. 25th IEEE Int. Conf. Micro Electro Mechanical Systems (MEMS),* pp. 1261–1264.

[19] J. I. Lee, Y. H. Jeong, H.-C. No, R. Hannebauer, and S.-K. Yoon, "Size effect of nanometer vacuum gap thermionic power conversion device with CsI coated graphite electrodes," *Appl. Phys. Lett.*, vol. 95, no. 22, pp. 223107, 2009.

[20] R. Yang, A. Narayanaswamy, and G. Chen, "Surface-plasmon coupled nonequilibrium thermoelectric refrigerators and power generators," *J. Comput. Theor. Nanosci.*, vol. 2, no. 1, pp. 75–87, 2005.

[21] Z. Taliashvili, A. Tavkhelidze, L. Jangidze, and Y. Blagidze, "Vacuum nanogap formation in multilayer structures by an adhesion-controlled process," *Thin Solid Films*, vol. 542, pp. 399–403, Sept. 2013.

[22] T. Zeng, "Thermionic-tunneling multilayer nanostructures for power generation," *Appl. Phys. Lett.*, vol. 88, no. 15, pp. 153104, 2006.

[23] S. F. Adams, "Solar thermionic space power technology testing: A historical perspective," in *Proc. Space Technology and Applications Int. Forum – STAIF 2006*, pp. 590-597.

[24] J. W. Schwede, I. Bargatin, D. C. Riley, B. E. Hardin, S. J. Rosenthal, Y. Sun, F. Schmitt, P. Pianetta, R. T. Howe, Z.-X. Shen, and N. A. Melosh, "Photon-enhanced thermionic emission for solar concentrator systems," *Nat. Mater.*, vol. 9, no. 9, pp. 762–767, 2010.

[25] K. L. Jensen, "General formulation of thermal, field, and photoinduced electron emission," *J. Appl. Phys.*, vol. 102, no. 2, p. 024911, 2007.

[26] R. H. Fowler, "The analysis of photoelectric sensitivity curves for clean metals at various temperatures," *Phys. Rev.*, vol. 38, no. 1, pp. 45–56, July 1931.

[27] L. A. DuBridge, "Theory of the energy distribution of photoelectrons," *Phys. Rev.*, vol. 43, no. 9, pp. 727–741, May 1933.

[28] K. Nakayama, K. Tanabe, and H. A. Atwater, "Plasmonic nanoparticle enhanced light absorption in GaAs solar cells," *Appl. Phys. Lett.*, vol. 93, pp. 121904, Sept. 2008.

[29] P. Yaghoobi, M. V. Moghaddam, and A. Nojeh, "'Heat trap': Light-induced localized heating and thermionic electron emission from carbon nanotube arrays," *Solid State Commun.*, vol. 151, no. 17, pp. 1105–1108, Sept. 2011.

[30] P. Yaghoobi, M. Vahdani Moghaddam, and A. Nojeh, "Solar electron source and thermionic solar cell," *AIP Adv.*, vol. 2, no. 4, pp. 042139–042139–12, Nov. 2012.

[31] R. C. O'Brien, R. M. Ambrosia, N. P. Bannistera, S. D. Howeb, and H. V. Atkinson, "Safe radioisotope thermoelectric generators and heat sources for space applications," *J. Nucl. Mater.*, vol. 377, no. 3, pp. 506–521, 2008.

[32] D. M. Rowe, Ed., *Thermoelectrics Handbook—Macro to Nano*, Boca Raton, FL: Taylor & Francis Group, 2006.

[33] A. F. Ioffe, *Semiconductor Thermoelements* and *Thermoelectric Cooling*, London: Infosearch Ltd., 1957.

[34] B. Bhushan, "Nanometer-scale thermoelectric materials," in *Springer Handbook of Nanotechnology*, 2nd ed., Springer, 2007, pp. 345-373.

[35] T. M. Tritt and M. A. Subramanian, "Thermoelectric materials, phenomena, and applications: A bird's eye view," *MRS Bull.*, vol. 31, no. 3, pp. 188–194, 2006.

[36] K. A. Chao and M. Larsson, "Thermoelectric phenomena from macro-systems to nano-systems," in *Physics of Zero- and One-Dimensional Nanoscopic Systems*, Springer, 2007, pp. 151–186.

[37] A. J. Minnich, et al., "Bulk nanostructured thermoelectric materials: Current research and future prospects," *Energy Env. Sci.*, vol. 2, pp. 466–479, Feb. 2009.

[38] G. A. Slack, "Nonmetallic crystals with high thermal conductivity," *J. Solid State Phys.*, vol. 34, no. 2, pp. 321–335, 1973.

[39] M. Christensen, et al., "Avoided crossing of rattler modes in thermoelectric materials," *Nature Mater.*, vol. 7, no. 10, pp. 811–815, 2008.

[40] M. M. Koza, M. R. Johnson, R. Viennois, H. Mutka, L. Girard, and D. Ravot, "Breakdown of phonon glass paradigm in La- and Ce-filled Fe_4Sb_{12} skutterudites," *Nature Mater.*, vol. 7, no. 10, pp. 805–810, Oct. 2008.

[41] P. Pichanusakorn and P. Bandaru, "Nanostructured thermoelectrics," *Mater. Sci. Eng. R*, vol. 67, nos. 2–4, pp. 19–63, Jan. 2010.

[42] M. S. Dresselhaus, G. Chen, M. Y. Tang, R. G. Yang, H. Lee, D. Z. Wang, Z. F. Ren, J.-P. Fleurial, and P. Gogna, "New directions for low-dimensional thermoelectric materials," *Adv. Mat.*, vol. 19, no. 8, pp. 1043–1053, Apr. 2007.

[43] H. Zhao, M. Pokharel, G. Zhu, S. Chen, K. Lukas, Q. Jie, C. Opeil, G. Chen, and Z. Ren, "Dramatic thermal conductivity reduction by nanostructures for large increase in thermoelectric figure-of-merit of $FeSb_2$," *Appl. Phys. Lett.*, vol. 99, no. 16, p. 163101, Oct. 2011.

[44] S. Maruyama, "A molecular dynamics simulation of heat conduction of a finite length single-walled carbon nanotube," *Microsc. Thermophys. Eng.*, vol. 7, no. 1, pp. 41–50, 2003.

[45] O. Narayan and S. Ramaswamy, "Anomalous heat conduction in one-dimensional momentum-conserving systems," *Phys. Rev. Lett.*, vol. 89, no. 20, pp. 200601-1–200601-4, 2002.

[46] E. Pop, D. Mann, Q. Wang, K. Goodson, and H. Dai, "Thermal conductance of an individual single-wall carbon nanotube above room temperature," *Nano Lett.*, vol. 6, no. 1, pp. 96–100, Jan. 2006.

[47] Y. W. Wen, H. J. Liu, L. Pan, X. J. Tan, H. Y. Lv, J. Shi, and X. F. Tang, "Reducing the thermal conductivity of silicon by nanostructure patterning," *App. Phys. A*, vol. 110, no. 1, pp. 93–98, Jan. 2013.

[48] A. I. Hochbaum, R. Chen, R. D. Delgado, W. Liang, E. C. Garnett, M. Najarian, A. Majumdar, and P. Yang, "Enhanced thermoelectric performance of rough silicon nanowires," *Nature Lett.*, vol. 451, no. 7175, pp. 163–167, Jan. 2008.

[49] A. I. Boukai, Y. Bunimovich, J. Tahir-Kheli, J.-K. Yu, W. A. Goddard Iii, and J. R. Heath, "Silicon nanowires as efficient thermoelectric materials," *Nano Lett.* vol. 451, no. 7175, pp. 168–171, Jan. 2008.

[50] K. Biswas, J. He, I. D. Blum, C.-I. Wu, T. P. Hogan, D. N. Seidman, V. P. Dravid, and M. G. Kanatzidis, "High-performance bulk thermoelectrics with all-scale hierarchical architectures," *Nature Lett.*, vol. 489, no. 7416, pp. 414–418, Sept. 2012.

N